MATHEMATICAL BIOSCIENCES
AND ENGINEERING
Volume **12**, Number **3**, June **2015**

doi:10.3934/mbe.2015.12.609

pp. **609–623**

OPTIMAL INFORMATION DISSEMINATION STRATEGY TO PROMOTE PREVENTIVE BEHAVIORS IN MULTILAYER EPIDEMIC NETWORKS

Heman Shakeri, Faryad Darabi Sahneh and Caterina Scoglio

Department of Electrical and Computer Engineering
Kansas State University
Manhattan, KS 66506-5204, USA

Pietro Poggi-Corradini

Department of Mathematics
Kansas State University
Manhattan, KS 66506-2602, USA

Victor M. Preciado

Department of Electrical and Systems Engineering
University of Pennsylvania
Philadelphia, PA 19104-6391, USA

(Communicated by Haiyan Wang)

Abstract. Launching a prevention campaign to contain the spread of infection requires substantial financial investments; therefore, a trade-off exists between suppressing the epidemic and containing costs. Information exchange among individuals can occur as physical contacts (e.g., word of mouth, gatherings), which provide inherent possibilities of disease transmission, and non-physical contacts (e.g., email, social networks), through which information can be transmitted but the infection cannot be transmitted. Contact network (CN) incorporates physical contacts, and the information dissemination network (IDN) represents non-physical contacts, thereby generating a multilayer network structure. Inherent differences between these two layers cause alerting through CN to be more effective but more expensive than IDN. The constraint for an epidemic to die out derived from a nonlinear Perron-Frobenius problem that was transformed into a semi-definite matrix inequality and served as a constraint for a convex optimization problem. This method guarantees a dying-out epidemic by choosing the best nodes for adopting preventive behaviors with minimum monetary resources. Various numerical simulations with network models and a real-world social network validate our method.

1. **Introduction.** Complications associated with modeling and analyzing epidemic spreading processes are well-studied problems. This paper focuses on mitigation of epidemic spreading, including consideration of available resources. Research in [7] and [8] showed that human behavior influences the spreading trend of an epidemic.

2010 *Mathematics Subject Classification.* Primary: 58F15, 58F17; Secondary: 53C35.

Key words and phrases. Epidemic spreading, awareness spreading, nonlinear Perron-Frobenius problem, convex optimization, asymptotic dying out.

This work has been partially supported by National Science Foundation by Award DMS-1201427.

These works introduced an extension of the "Susceptible-Infected-Susceptible" (SIS) model by adding an "Alert" state that incorporates preventive behavior. Sahneh *et al.* revealed an operating region in which the infection eventually dies out due to cautious behavior of people exposed to infected neighbors. Consequently, if an epidemic is stronger than the SIS classical threshold, long-term disease elimination is possible after a break-out period.

Sun *et al.* used an SI model to study causes of disease extinction, such as infection rate and migration [25]. In [24], Sun studied disease transmission and spatial patterns of spreading with nonlinear incidence rates. He demonstrated the positive correlation of force of infection β on these patterns.

Granell *et al.* studied interplay between disease and information in a two-layer network consisting of one physical contact network that spread the disease and a virtual overlay network that spread information to mitigate the disease [14]. They found a meta-critical point for the epidemic depending on awareness dynamics and the overlay network structure.

A majority of works concerning epidemic models have been conducted on a single graph. However, the study of disease spread in physical systems requires an elaborate interaction model based on multiple interconnected networks ([12], [10], [22], and [28]). [3] contains a comprehensive review on structural and dynamical organization of multilayer networks.

Sahneh *et al.* extended their analysis for multilayer networks in [9] by considering an additional directed network layer with nodes identical to the contact network (CN) but with different edges between these nodes. Information exchange was realized through these networks and each individual became aware of the state of infected neighbors at rates proportional to the number of neighbors. They proposed an optimal structure for information dissemination network (IDN) by introducing an information dissemination metric.

Preciado *et al.* controlled the spreading process by investing in alertness rates using the "Susceptible-Alert-Infected-Susceptible" (SAIS) model and considering some realistic assumptions on the cost function in order to obtain a convex optimization framework. In [21], Preciado *et al.* attempted to ensure that largest eigenvalue was smaller than the persisting threshold introduced in [8], consequently leading to rate control based on CN structure.

Motivated by [21] and using threshold concepts in [8] and [7], we attempted to identify alertness rates on multilayer networks in order to achieve a dying-out epidemic. However this problem is more general than [9] because each layer can have an arbitrary structure. The second threshold was obtained from a nonlinear eigenvalue problem that is a nonlinear form of the Perron-Frobenius problem. In order to obtain optimal rates, we coupled this nonlinear Perron-Frobenius problem (NPF) with a convex optimization problem, creating a general method that can be applied to solve a variety of optimization problems combined with NPF problems in various disciplines. Optimal rates were obtained for a specific effective infection rate, so epidemics with identical or weaker effective infection rates will certainly die-out with a safety margin. In addition, by monitoring the status of a small subgroup and characterizing epidemic properties and behavioral response, we obtained a cost effective strategy to mitigate long run spreading for the entire population.

The remainder of the paper is organized as follows. In Section 2, we introduce our notation and modeling method and we analyze characteristics of the multilayer

model. In Section 3, we introduce problem statements, and in Section 4 we demonstrate how to approach this problem, proving necessary properties and introducing the coupled NPF problem with the convex problem. In Section 5, we solve several examples of standard networks and a real-world network and discuss results.

2. Model development.

2.1. Graph theory preliminaries.

Graph theory is used to represent contact topology in an epidemic network [11]. Using the same notations and assumptions as in [9], $\mathcal{G} = \{\mathcal{V}, \mathcal{E}\}$ represents a graph and $\mathcal{V} = \{1, \ldots, N\}$ denotes the set of vertices. The set of edges is denoted by $\mathcal{E} \subset \mathcal{V} \times \mathcal{V}$, and each edge is an ordered pair $(i, j) \in \mathcal{E}$.

2.2. Multilayer Network structure.

We used a multilayer network structure to represent multiple types of interconnection among individuals in the population. A multilayer network consists of L layers of graphs that have identical nodes but their edges can be different and independently formed. In this work, we considered a two-layer network. Although a disease can propagate among individuals through the physical contact network (CN), information can spread among the same individuals through an on-line information dissemination network (IDN).

Since physical interactions can be considered as undirected edges and we omit individuals who do not interact with the population, therefore, these assumptions lead to an undirected and connected graph for CN. Some people may not have a social network account or a person may follow a celebrity on Twitter but that celebrity does not reciprocate; therefore, IDN can be directed and not connected.

$A = [a_{ij}] \in \mathbb{R}^{N \times N}$ denotes the adjacency matrix of CN, where $a_{ij} = 1$ if and only if $(i, j) \in \mathcal{E}$; otherwise $a_{ij} = 0$. Similarly, we defined the adjacency matrix of IDN as $B = [b_{ij}]_{N \times N}$. The largest eigenvalue of the adjacency matrix A, known as the spectral radius of A, is denoted by $\lambda_1(A)$; elements of the corresponding eigenvector v_1 are real and non-negative. Spectral centrality of nodes in a graph is determined by the rank of corresponding elements of v_1.

2.3. Model development.

In this paper, results are based on the SAIS model developed in [8]. Each node is allowed to be in one of three states: *'susceptible'*, *'infected'*, or *'alert'* and a node maintained the same state in all layers. A susceptible node becomes infected with a given infection rate through infected neighbors in CN and becomes alert through infected neighbors in different layers with corresponding rates. An alert node becomes infected with a rate less than the initial infection rate. An infected node is recovered at a given removing/recovery rate. For each agent $i \in \{1, ..., N\}$, let the random variable $x_i(t) = e_1$, if the agent i is susceptible at time t, $x_i(t) = e_2$ if alert, and $x_i(t) = e_3$ if infected, where $e_1 = [1, 0, 0]^T$, $e_2 = [0, 1, 0]^T$, and $e_3 = [0, 0, 1]^T$ are standard unit vectors of $\mathbb{R}^3$. Throughout this paper, the infection rate for an alert individual is assumed to be a reduced version of β, i.e., $r\beta$ with $r \leq 1$.

In the following equations, $\Pr[\cdot]$ denotes probability, $X(t) \triangleq \{x_i(t), i = 1, ..., N\}$ is the joint state of the network, $\Delta t > 0$ is a time step, and the indicator function $1_{\{\mathcal{X}\}}$ is 1 if $\mathcal{X}$ is true and 0 otherwise. A function $f(\Delta t)$ is said to be $o(\Delta t)$ if $\lim_{\Delta t \to 0} \frac{f(\Delta t)}{\Delta t} = 0$. For node i, $Y_i(t)$ is the number of neigbors in CN who are infected at time t and Z_i is the number of neigbors in IDN who are infected at time

t:

$$Y_i(t) \triangleq \sum_{j=1}^{N} a_{ij} 1_{\{x_j(t)=e_3\}},$$

$$Z_i(t) \triangleq \sum_{j=1}^{N} b_{ij} 1_{\{x_j(t)=e_3\}}.$$

There are four stochastic transitions in the SAIS model:

1. A susceptible agent becomes infected with infection rate β times the number of infected neighbors:
$$\Pr[x_i(t+\Delta t) = e_3 | x_i(t) = e_1, X(t)] = \beta Y_i(t)\Delta t + o(\Delta t), \quad (1)$$
for $i \in \{1, ..., N\}$.
2. An infected agent recovers to the susceptible state with curing rate δ:
$$\Pr[x_i(t+\Delta t) = e_1 | x_i(t) = e_3, X(t)] = \delta\Delta t + o(\Delta t). \quad (2)$$
3. A susceptible agent may become alert if surrounded by infected individuals in both CN and IDN. Specifically, a susceptible node becomes alert with alerting rate $\kappa \in \mathbb{R}^+$ times the number of infected neighbors in CN and with alerting rate $\mu \in \mathbb{R}^+$ times the number of infected neighbors in IDN:
$$\Pr[x_i(t+\Delta t) = e_2 | x_i(t) = e_1, X(t)] = (\kappa_i Y_i(t) + \mu_i Z_i(t))\Delta t + o(\Delta t), \quad (3)$$
4. An alert agent can become infected but with a weaker infection rate $0 < r\beta < \beta$:
$$\Pr[x_i(t+\Delta t) = e_3 | x_i(t) = e_2, X(t)] = r\beta Y_i(t)\Delta t + o(\Delta t). \quad (4)$$

Stochastic compartmental transitions of a node are depicted in Figure 1-a. An Illustrative schematic of CN and IDN is shown in Figure 1-b.

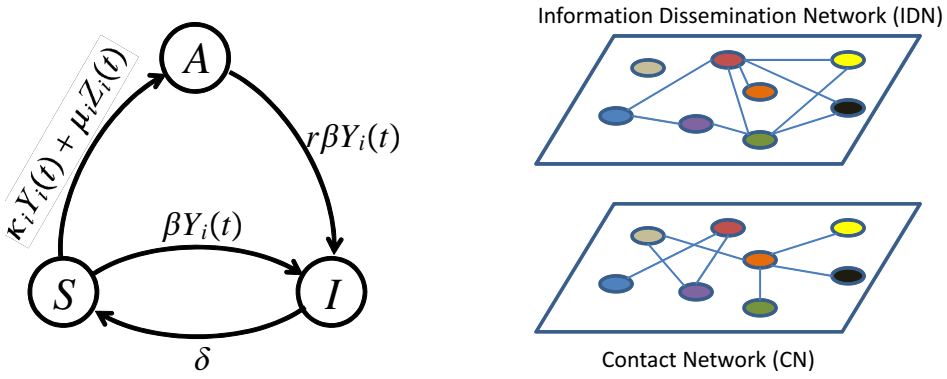

FIGURE 1. From left to right, (a) Compartmental transition graph according to the SAIS model with information dissemination. Y_i and Z_i are the number of infected neighbors of agent i in contact network and information dissemination network, respectively [9]; (b) Multilayer contact topology.

Let p_i and q_i denote the probabilities that agent i is and alert, respectively. The SAIS model with the information dissemination layer is obtained with some

modification from [9]:

$$\dot{p}_i = \beta\,(1 - p_i - q_i)\sum_{j=1}^{N} a_{ij}p_j + r\beta q_i \sum_{j=1}^{N} a_{ij}p_j - \delta p_i; \tag{5}$$

$$\dot{q}_i = (1 - p_i - q_i)\left\{\kappa_i \sum_{j=1}^{N} a_{ij}p_j + \mu_i \sum_{j=1}^{N} b_{ij}p_j\right\} - r\beta q_i \sum_{j=1}^{N} a_{ij}p_j. \tag{6}$$

Equations (5) and (6) are derived by a mean field Type approximation [26].

2.4. **Analysis of SAIS model.**

2.4.1. *SAIS with no alertness (SIS).* When no alertness transmission is present through CN or IDN, $\kappa_i = 0$ and $\mu_i = 0$, the model reduced to the original SIS model, as discussed in [7]. Therefore, the system exhibits a threshold for the effective infection rate $\tau \triangleq \frac{\beta}{\delta}$, under which the infection dies out exponentially. This threshold has been proven to be the inverse of the largest eigenvalue of CN adjacency matrix in $\tau_{c_1} \triangleq \frac{1}{\lambda_1(A)}$ ([13], [5], and [27]).

2.4.2. *SAIS with alertness dissemination.*

Theorem 2.1. *In the SAIS model (5-6), initial infections will die out exponentially if the effective infection rate τ is less than $\tau_{c_1} = \lambda_1^{-1}$ and a second threshold, τ_{c_2}, exists such that if $\tau_{c_1} < \tau < \tau_{c_2}$, then the infection dies out asymptotically after an initial spread. In addition, the second threshold $\tau_{c_2}(\kappa_i, \mu_i)$ is a monotonically increasing function of κ_i and μ_i.*

Proof. [9] contains the proof. □

The first threshold depends only on topology of the CN layer, but the second threshold depends on behavioral properties and topology of both layers.

After the second threshold, i.e., $\tau > \tau_{c_2}$, steady-state values of infection probabilities are positive and τ_{c_2} can be determined by studying the steady-state solution. According to (5) and (6), at the steady-state,

$$(1 - p_i^*)\left\{\kappa_i \sum_{j=1}^{N} a_{ij}p_j^* + \mu_i \sum_{j=1}^{N} b_{ij}p_j^*\right\} - q_i^*\left\{\kappa \sum_{j=1}^{N} a_{ij}p_j^* + k\sum_{j=1}^{N} b_{ij}p_j^*\right\} - r\beta q_i^* \sum_{j=1}^{N} a_{ij}p_j^* = 0; \tag{7}$$

$$q_i^* = (1 - p_i^*)\frac{\bar{\kappa}_i \sum_{j=1}^{N} a_{ij}p_j^* + \bar{\mu}_i \sum_{j=1}^{N} b_{ij}p_j^*}{(1 + \bar{\kappa}_i)\sum_{j=1}^{N} a_{ij}p_j^* + \bar{\mu}_i \sum_{j=1}^{N} b_{ij}p_j^*}, \tag{8}$$

where p_i^* and q_i^* are steady-state probabilities and $\bar{\kappa}_i \triangleq \frac{\kappa_i}{r\beta}$ and $\bar{\mu} \triangleq \frac{\mu}{r\beta}$ are normalized alertness rates. Combining (7) and (8), the steady-state equation becomes,

$$\tau(1 - p_i^*)\sum_{j=1}^{N} a_{ij}p_j^*$$

$$-\tau(1-r)(1-p_i^*)\frac{\bar{\kappa}_i\sum_{j=1}^N a_{ij}p_j^*+\bar{\mu}_i\sum_{j=1}^N b_{ij}p_j^*}{(1+\bar{\kappa}_i)\sum_{j=1}^N a_{ij}p_j^*+\bar{\mu}_i\sum_{j=1}^N b_{ij}p_j^*}\sum_{j=1}^N a_{ij}p_j^* = p_i^*. \quad (9)$$

Theorem 2.2. *The second threshold is the nontrivial solution of the following nonlinear eigenvalue problem:*

$$\tau_{c_2} diag\left(\frac{(1+r\bar{\kappa}_i)\sum_{j=1}^N a_{ij}w_j+r\bar{\mu}_i\sum_{j=1}^N b_{ij}w_j}{(1+\bar{\kappa}_i)\sum_{j=1}^N a_{ij}w_j+\bar{\mu}_i\sum_{j=1}^N b_{ij}w_j}\right)A_{\mathcal{G}}\mathbf{w}=\mathbf{w}, \quad (10)$$

where $\mathbf{w}=[w_1,...,w_N]^T$, *with* $w_i>0 \quad \forall i=1,...,N$.

Proof. Define $\tilde{\tau}\triangleq\tau-\tau_{c_2}$. Close to the second threshold, i.e., as $\tilde{\tau}\to 0^+$, we have $p_i^*=\tilde{\tau}\frac{\partial p_i^*}{\partial\tau}|_{\tau=\tau_{c_2}}+o(\tilde{\tau})$. Letting $\tau\to\tau_{c_2}^+$ in (9),

$$\tau_{c_2}\sum_{j=1}^N a_{ij}\frac{\partial p_j^*}{\partial\tau}|_{\tau=\tau_{c_2}} - \tau_{c_2}(1-r)\frac{\bar{\kappa}_i\sum_{j=1}^N a_{ij}\frac{\partial p_j^*}{\partial\tau}|_{\tau=\tau_{c_2}}+\bar{\mu}_i\sum_{j=1}^N b_{ij}\frac{\partial p_j^*}{\partial\tau}|_{\tau=\tau_{c_2}}}{(1+\bar{\kappa}_i)\sum_{j=1}^N a_{ij}\frac{\partial p_j^*}{\partial\tau}|_{\tau=\tau_{c_2}}+\bar{\mu}_i\sum_{j=1}^N b_{ij}\frac{\partial p_j^*}{\partial\tau}|_{\tau=\tau_{c_2}}} \sum_{j=1}^N a_{ij}\frac{\partial p_j^*}{\partial\tau}|_{\tau=\tau_{c_2}} = \frac{\partial p_i^*}{\partial\tau}|_{\tau=\tau_{c_2}}. \quad (11)$$

Because τ_{c_2} is the second threshold, $\frac{\partial p_i^*}{\partial\tau}|_{\tau=\tau_{c_2}}$ must be positive for every $i\in\{1,...,N\}$. Therefore, τ_{c_2} is such that the set of algebraic equations (10) has positive solutions. By substituting $w_j=\frac{\partial p_j^*}{\partial\tau}|_{\tau=\tau_{c_2}}$ in (11), the nonlinear eigenvalue problem in (10) can be obtained. □

3. **Problem statement.** Given network layer adjacency matrices A and B and disease properties β, δ, and r, the following optimization problem is considered:

$$\begin{aligned}\underset{\bar{\kappa}_i,\bar{\mu}_i}{\text{minimize}} \quad & \sum_{i=1}^N f_i(\bar{\kappa}_i,\bar{\mu}_i)\\ \text{subject to} \quad & \tau_{c_2}(\bar{\kappa}_i,\bar{\mu}_i)\geq\tau,\\ & \bar{\mu}_{min}\leq\bar{\mu}_i\leq\bar{\mu}_{max},\\ & \bar{\kappa}_{min}\leq\bar{\kappa}_i\leq\bar{\kappa}_{max}.\end{aligned} \quad (12)$$

where f_i is a linear fractional cost function to promote alertness in the population [21]. Minimization of this objective function while constraining the system to die out asymptotically, requires a trade-off.

Asymptotic stability constraint. According to Theorem 2.1, in order to have an asymptotically dying-out infection, the effective infection rate should be less than the second threshold, corresponding to the first constraint in (12).

The nonlinear eigenvalue problem in (10) can be written as follows:

$$diag\left(h_i(\boldsymbol{\xi}_i,\mathbf{w})\right)A\mathbf{w}=\lambda\mathbf{w}, \quad (13)$$

where $diag\left(h_i\left(\boldsymbol{\xi}_i, \mathbf{w}\right)\right)$ is a nonnegative diagonal matrix with unknown parameters $\boldsymbol{\xi}_i = [\bar{\kappa}_i, \bar{\mu}_i]\,, \quad \forall i = 1, ..., N$ and λ corresponds to the inverse of the second threshold τ_{c_2}. Therefore the eigenvalue problem in (13) is a NPF problem [17].

According to NPF theory, the largest eigenvalue is positive and real and the corresponding normalized eigenvector $\mathbf{w}$ is unique and positive [17].

4. **Solution methodology.** Given $\boldsymbol{\xi}_i$ using the power iteration algorithm, the largest eigenvalue and corresponding eigenvector of (13) can be found. Starting with an initial guess for $\mathbf{w^{(0)}}$, the following iteration is performed:

$$diag\left(h_i\left(\boldsymbol{\xi}_i, \mathbf{w}^{(l)}\right)\right) A\mathbf{w}^{(l)} = \lambda^{(l+1)}\mathbf{w}^{(l+1)}, \tag{14}$$

where $\lambda^{\mathbf{(k+1)}}$ and $\mathbf{w^{(k+1)}}$ are the approximated value of the largest eigenvalue and corresponding eigenvector in the k'th step. They are obtained from the following relations:

$$\lambda^{(l+1)} = \| \; diag\left(h_i\left(\boldsymbol{\xi}_i, \mathbf{w}^{(l)}\right)\right) A\mathbf{w}^{(l)} \; \|; \tag{15}$$

$$\mathbf{w}^{(l+1)} = \frac{diag\left(h_i\left(\boldsymbol{\xi}_i, \mathbf{w}^{(l)}\right)\right) A\mathbf{w}^{(l)}}{\| \; diag\left(h_i\left(\boldsymbol{\xi}_i, \mathbf{w}^{(l)}\right)\right) A\mathbf{w}^{(l)} \; \|}. \tag{16}$$

This algorithm has guaranteed convergence to the largest eigenvalue and corresponding eigenvector of (13) with a chosen tolerance ε [1]. Pseudocode for this algorithm is given in Algorithm 1.

Algorithm 1 Power iteration

Input guess$\leftarrow \mathbf{w^{(0)}}$
Output: $\mathbf{w} = \mathbf{w}^{(l+1)}$
1: **for** l **do**
2: $\quad \mathbf{w}^{(l)} \leftarrow$guess
3: $\quad \mathbf{w}^{(l+1)} = \frac{diag\left(h_i\left(\boldsymbol{\xi}_i, \mathbf{w}^{(l)}\right)\right) A\mathbf{w}^{(l)}}{\| diag\left(h_i\left(\boldsymbol{\xi}_i, \mathbf{w}^{(l)}\right)\right) A\mathbf{w}^{(l)} \|}$
4: $\quad$ **if** $\mid \mathbf{w}^{(l+1)} - \mathbf{w}^{(l)} \mid \leq \varepsilon$ **then**
5: $\quad\quad$ stop
6: $\quad$ **end if**
7: $\quad$ guess$\leftarrow \mathbf{w}^{(l+1)}$
8: **end for**

Proposition 1. *Optimal parameters in (10) can be found by alternating between the NPF problem and the optimization problem.*

Proof. Starting with a guess for $\boldsymbol{\xi}_i^{(0)}$,

$$diag\left(h_i\left(\boldsymbol{\xi}_i^{(0)}, \mathbf{w}\right)\right) A\mathbf{w} = \lambda\mathbf{w}. \tag{17}$$

Using the derived eigenvector $\mathbf{w^{(0)}}$ from the power method, we approximate $diag\left(h_i\left(\boldsymbol{\xi}_i, \mathbf{w}\right)\right)$ as $diag\left(h_i\left(\boldsymbol{\xi}_i, \mathbf{w}^{(0)}\right)\right)$ and then solve the optimization problem in (12), and find new approximation for parameters $\boldsymbol{\xi}_i^{(1)}$ as the new guess. Because of existing constraints, new obtained parameters ensure initial NPF problem properties. Using the updated guess, we alternate between the NPF problem and the optimization problem until these guesses converges with a tolerance ϵ, i.e., $\mid \boldsymbol{\xi}_i^{(k)} - \boldsymbol{\xi}_i^{(k-1)} \mid \leq \epsilon$. □

At each step with approximated $diag\left(h_i\left(\boldsymbol{\xi}_i, \mathbf{w}^{(k)}\right)\right)$, the NPF problem in 10 becomes a linear Perron-Frobenius problem. Therefore, the first constraint in (12) transforms to a semidefinite inequality with the following lemma.

Lemma 4.1. *If D is a diagonal matrix with positive diagonal entries, A is a symmetric matrix, τ_c and τ are scalars, and the following eigenvalue problem exists:*

$$\tau_c DAw = w, \tag{18}$$

for $\tau \leq \tau_c$:

$$A - (\tau D)^{-1} \preceq 0. \tag{19}$$

Proof. First, we show that eigenvalues of $\tau_c DA$ are real with the following variable change:

$$w = D^{\frac{1}{2}} x. \tag{20}$$

Rewriting (18),

$$\tau_c DAD^{\frac{1}{2}} x = D^{1/2} x, \tag{21}$$

and multiplying both sides by $D^{-\frac{1}{2}}$ produces

$$\tau_c D^{\frac{1}{2}} AD^{\frac{1}{2}} x = x, \tag{22}$$

which shows that DA and $D^{\frac{1}{2}} AD^{\frac{1}{2}}$ share similar eigen-properties. Then, since $D^{\frac{1}{2}} AD^{\frac{1}{2}}$ is symmetric, it has real eigenvalues; therefore, DA also has real eigenvalues.

From (18):

$$\lambda_1 (\tau_c DA) = 1. \tag{23}$$

If $\tau \leq \tau_c$

$$\tau \lambda_1 (DA) - 1 \leq 0,$$

which can be rewritten as

$$\lambda_1 (\tau DA - I) \leq 0. \tag{24}$$

Equations (24) and (22) show that

$$\left(\tau D^{\frac{1}{2}} AD^{\frac{1}{2}} - I\right) \preceq 0, \tag{25}$$

or

$$A - (\tau D)^{-1} \preceq 0. \tag{26}$$

□

Convex formulation. According to Lemma 4.1, the dying-out constraint, $\tau_{c_2}(\bar{\kappa}_i, \bar{\mu}_i) \geq \tau = \frac{\beta}{\delta}$ can be written as,

$$A - \frac{\delta}{\beta} diag\left(\frac{(1+\bar{\kappa}_i)\phi_i^A + \bar{\mu}_i \phi_i^B}{(1+r\bar{\kappa}_i)\phi_i^A + r\bar{\mu}_i \phi_i^B}\right) \preceq 0, \tag{27}$$

where ϕ_i^A and ϕ_i^B represent $\sum_{j=1}^N a_{ij} w_j$ and $\sum_{j=1}^N b_{ij} w_j$, respectively. For a linear fractional cost function,

$$\sum_{i=1}^N \frac{c_i \bar{\kappa}_i + t_i \bar{\mu}_i}{r\bar{\kappa}_i \phi_i^A + r\bar{\mu}_i \phi_i^B + \phi_i^A}, \tag{28}$$

the problem in (12) is a quasiconvex optimization problem [4].

Because all equations are homogeneous, we choose a scale z_i such that for $i \in 1, \cdots, N$, $z_i \left(r\bar{\kappa}_i\phi_i^A + r\bar{\mu}_i\phi_i^B + \phi_i^A\right) = 1$. Substituting[1] $u_i = z_i\bar{\kappa}_i$ and $v_i = z_i\bar{\mu}_i$ produced the following semi-definite optimization problem (SDP) equivalent to (12):

$$\begin{aligned} \underset{u_i,v_i,z_i}{\text{minimize}} \quad & \sum_{i=1}^{N} \left(c_i u_i + t_i v_i\right) \\ \text{subject to} \quad & A - \frac{\delta}{\beta} diag\left(u_i\phi_i^A + v_i\phi_i^B + z_i\phi_i^A\right) \preceq 0, \\ & rU\Phi^A + rV\Phi^B + Z\Phi^A = I, \\ & \bar{\mu}_{min} z_i \leq u_i \leq \bar{\mu}_{max} z_i, \\ & \bar{\kappa}_{min} z_i \leq v_i \leq \bar{\kappa}_{max} z_i. \end{aligned} \tag{29}$$

where U, V, Z, Φ^A, and Φ^B are diagonal matrices with u_i, v_i, z_i, ϕ_i^A and ϕ_i^B as their entries, respectively. Using classic solvers such as interior point-based methods, the SDP in (29) can be solved in a fast and robust fashion for networks up to 1000 nodes [19]. In this work, we use CVX [15]. Subgradient methods [16] or smoothing and accelerated algorithms [18] can be used to efficiently solve (29) in very large networks. These methods are well-studied and powerful commercial solvers are developed for applying them.

From Proposition 1, Φ^A and Φ^B update with each iteration and carry new structural properties; therefore, a new optimization problem should be solved each time causing $\bar{\kappa}_i$, $\bar{\mu}_i$, and w_i to converge to the desired solution. Pseudocode is given in Algorithm 2.

Algorithm 2 Power iteration

Input guess$\leftarrow \boldsymbol{\xi}_i^{(0)}$
Output: $\boldsymbol{\xi} = \boldsymbol{\xi}_i^{(k)}$
for k **do**
  $\boldsymbol{\Phi}^{\mathbf{A}(k)}, \boldsymbol{\Phi}^{\mathbf{B}(k)} \leftarrow$Power method
  Convex Problem$\leftarrow \boldsymbol{\Phi}^{\mathbf{A}(k)}, \boldsymbol{\Phi}^{\mathbf{B}(k)}$
  $\boldsymbol{\xi}_i^{(k)} \leftarrow$Convex Problem
  if $\mid \boldsymbol{\xi}_i^{(k)} - \boldsymbol{\xi}_i^{(k-1)} \mid \leq \epsilon$ **then**
    stop
  end if
  guess$\leftarrow \boldsymbol{\xi}_i^{(k)}$
end for

5. **Numerical simulations.** We considered an infectious disease with an effective infection rate $\frac{\beta}{\delta} = \frac{3}{\lambda_1(A)}$, an unstable situation in SIS, and a reduction in infection rate $r = \frac{1}{3}$ due to alertness. Alertness rates vary between an upper limit and a lower limit, based on response capacity of the population. Due to inherent differences between μ_i and κ_i, a higher awareness may be reached through CN, but these rates are more expensive than rates in IDN. In the following simulations, we assume that $\mu_{max} = 5$, $\kappa_{max} = 10$, and $\mu_{min} = \kappa_{min} = 0$, and cost function weights are $c = 1.5$ and $t = 1$.

[1]This transformation is similar to Charnes-Cooper transformation [6].

For the following multilayer structures, if no information dissemination is available the second threshold does not exist and dying-out epidemic occurs if $\frac{\beta}{\delta} < \frac{1}{\lambda_1(A)}$. Considering information dissemination through CN and without IDN, if we assign the highest amount of alertness rate for all individuals, i.e., $\kappa_i = \kappa_{max}$, then $\tau_{c_2}\left(\kappa_i = \kappa_{max}, \mu_i = 0\right) = \frac{1+\kappa_{max}}{1+r\kappa_{max}} \frac{1}{\lambda_1(A)} = 2.51 \frac{1}{\lambda_1(A)}$ which cannot suppress the epidemic even though it is very expensive. However, use of IDN and proposed optimal rates helps achieve a cost-efficient suppression of the epidemic.

In the following simulations, we selected a preferential attachment network [2] for IDN. Four networks were selected for CN: a regular random network, a geometric random network [20], a preferential attachment network, and a real-world social (face-to-face) network.

Example 1: CN is a regular random graph. In this example, the CN layer is a regular random graph. Nodes in a regular graph has the same number of neighbors. Obtained optimal alertness rates are depicted in Figure 2.

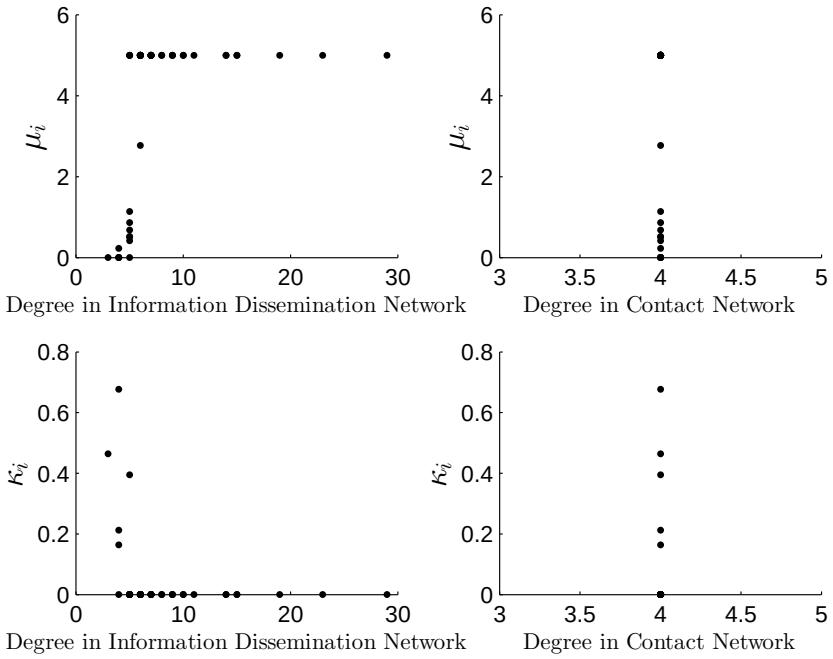

FIGURE 2. Optimal alertness rates μ_i and κ_i for $i = 1, \cdots, 50$, with respect to degree of nodes in both layers. Each layer has 50 nodes. The information dissemination network is a preferential attachment network with minimum node degree 5, and the contact network has a random regular structure with node degree 4. *Note:* There are nodes with the same node degree and same optimum rates which caused overlapping in the figure.

Because all individuals have identical number of neighbors in CN, the only difference between them is their degree in IDN. For individuals with high degree, μ_i

influence is more effective compared to lower degree nodes. Since promotion of μ_i is less expensive than κ_i, maximum investment of μ_i is optimum after a certain degree (nodes with $deg_i \geq 6$ in this example) in IDN. For nodes with lower degree in IDN, more reliable sources of information are neighbors in CN, similar to occasions when people are not active in online social networks and must be contacted through their neighbors in CN. In this example, since promoting alertness in CN is more expensive, although $\kappa_{max} > \mu_{max}$, the optimization problem does not allow any node to have $\kappa_i = \kappa_{max}$ while $\mu_i = \mu_{max}$.

Example 2: CN is a random geometric graph. In this example, CN is a random connected geometric graph in a two-dimensional coordinate system. Optimal alerting rates versus degree in both layers are shown in Figure 3. Because high degree nodes in CN mean increased exposure to the infection, a high emphasis must be assigned to them. Furthermore, low degree in CN means decreased infecting opportunities and, because of limited monetary resources, the proposed method allocates all available resources to higher degree nodes. Unlike Example 1, some nodes are assigned with the maximum amount of κ_i. Nodes with $\mu_i = \mu_{max}$ and $\kappa_i = \kappa_{max}$ (saturated nodes) are hubs in IDN and high degree nodes in CN.

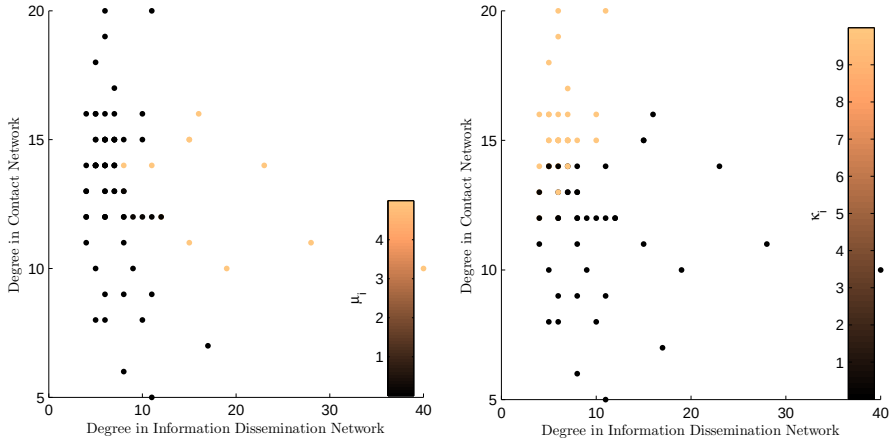

FIGURE 3. Alertness rates μ_i and κ_i for $i = 1, \cdots, 80$, with respect to degree of each nodes in both layers. Each layer has 80 nodes. The IDN is a preferential attachment network with minimum node degree 5, and the contact network has a random geometric structure. *Note:* Colors represent the optimum rates according to the colorbar. Nodes with identical node degree caused overlapping in the figure.

Example 3: CN is a random preferential attachment network. In this example, both layers are preferential attachment networks with different preferential attachment probabilities and 80 nodes. Optimal alerting rates as a function of node degree in both layers are shown in Figure 4. Similar to previous examples investment on very low degree individuals in the presence of financial restrictions is not wise. Since high degree nodes in CN are more exposed to the infection, they must be

encouraged to be alert through IDN or CN neighbors. Results identical to example 2 can be observed. Emphasis on high degree individuals is notable (hubs).

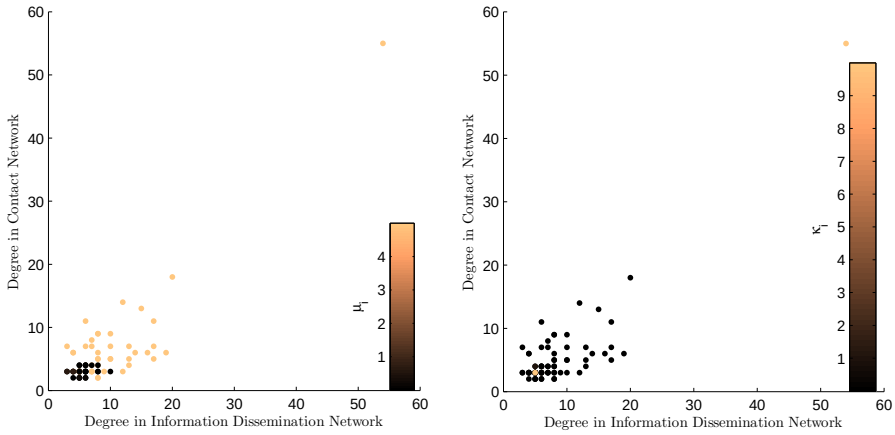

FIGURE 4. Alertness rates μ_i and κ_i for $i = 1, \cdots, 80$, with respect to degree of each nodes in both layers. Each layer has 80 nodes. The IDN is a preferential attachment network with minimum node degree 5, and the contact network has a preferential network with minimum node degree 3. *Note:* Colors represent the optimum rates according to the colorbar. Nodes with identical node degree caused overlapping in the figure.

Example 4: CN is a social (face-to-face) network. In this example, the CN layer is a portion of the social contact network based on survey of a community in Chanute, Kansas, United States [23]. In an effort to consider important connections in the network, we remove links with weights less than 0.2. Based on weight distribution in [23], we consider the remining connected network as an unweighted CN with 102 nodes (Figure 5).

Similar to previous examples a preferential attachment network as IDN with the same size as CN is considered. Optimal alerting rates as a function of node degree in both layers are shown in Figure 6. Results identical to the previous examples are observed. In addition, for nodes with high degree in CN or more exposed to the infection, optimal alertness investments are either through CN or IDN. An extreme case, such as a hub, that must be considered from both networks was not observed in this example.

The threshold phenomena predicted in [21] is observed in these examples too. Because of effects from IDN, this threshold is not abrupt. In order to determine optimal alertness rates, a transition zone exists with a trade-off between topological characteristics of both layers.

6. **Conclusions.** Based on the SAIS epidemic model, containment and suppression of an infectious disease spreading in a CN are possible with the help of disease-awareness diffusion among individuals. We proposed a method to optimally allocate

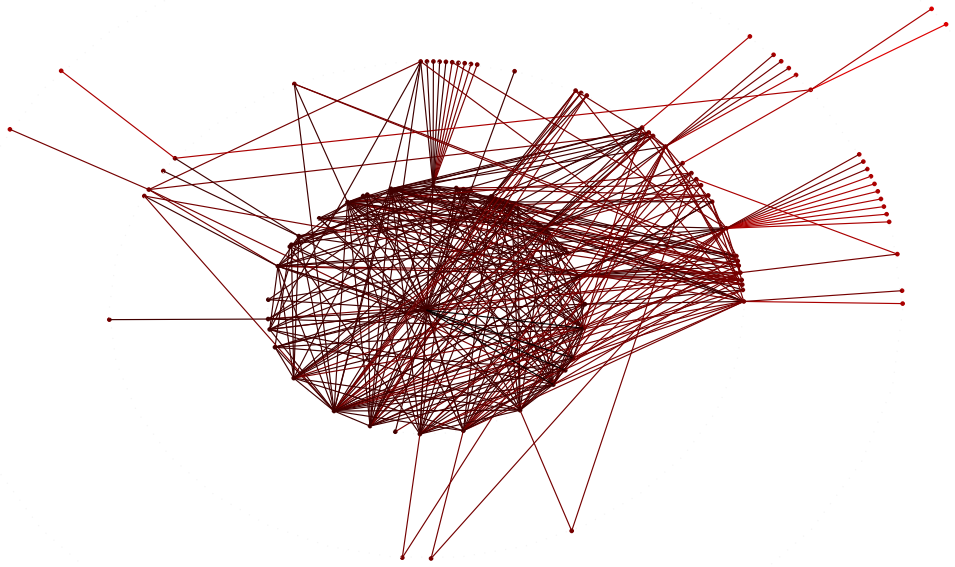

FIGURE 5. A portion of the social (face-to-face) network built based on a survey of a community in Chanute, Kansas, United States [23]. Network size is 102, maximum node degree is 36, and minimum node degree is 1

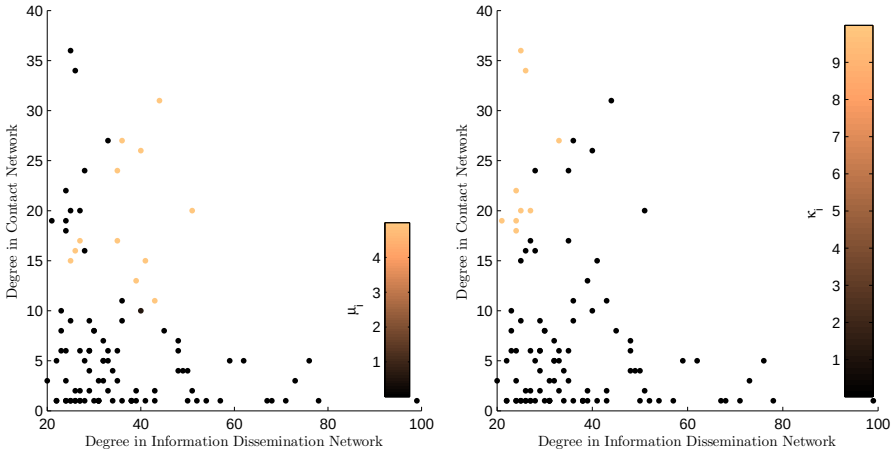

FIGURE 6. Alertness rates μ_i and κ_i $i = 1, \cdots, 102$, with respect to degree of each nodes in both layers. Each layer has 102 nodes. The IDN is a preferential attachment network with minimum node degree 20, and the contact network is a portion of a rural county social (face-to-face) network [23]. *Note:* Colors represent the optimum rates according to the colorbar. Nodes with identical node degree caused overlapping in the figure.

available monetary resources for disease awareness. In particular, we determined optimal transition rates to a preventive-behavior state for each individual in the CN and IDN layers. We demonstrated that an epidemic can be contained in a multilayer network structure for a larger range of effective infection rates compared to a one-layer structure with the identical amount of resources. Furthermore, by allocating resources in both layers, epidemics can be contained that cannot be contained in a one-layer structure with more resources. Awareness rates are obtained by alternating the solution of a NPF problem and a convex optimization problem for an epidemic with a given effective infection rate until convergence is obtained. These optimum rates are positively correlated with node degrees in both layers. Therefore, any epidemic with identical or weaker effective infection rate is suppressed with a safety margin. This method selects the best individuals for adopting preventive behaviors with minimal costs and guaranteed epidemic dying-out.

REFERENCES

[1] O. Axelsson, *Iterative Solution Methods*, Cambridge University Press, 1994.

[2] A. L. Barabasi and R. Albert, Emergence of Scaling in Random Networks, *Science*, **286** (1999), 509–512.

[3] S. Boccaletti, G. Bianconi, R. Criado, C. I. del Genio, J. Gómez-Gardeñes, M. Romance, I. Sendiña-Nadal, Z. Wang and M. Zanin, The structure and dynamics of multilayer networks, in *Physics Reports*, **544** (2014), 1–122.

[4] S. Boyd and L. Vandenberghe, *Convex Optimization*, Cambridge University Press, 2004.

[5] D. Chakrabarti, Y. Wang, C. Wang, J. Leskovec and C. Faloutsos, Epidemic Thresholds in Real Networks, *ACM Trans. Inf. Syst. Secur.*, **10** (2008), 1–26.

[6] A. Charnes and W. W. Cooper, Programming with linear fractional functionals, *Naval Research Logistics*, **9** (1962), 181–186.

[7] F. Darabi Sahneh, F. N. Chowdhury and C. Scoglio, *On the Existence of a Threshold for Preventive Behavioral Responses to Suppress Epidemic Spreading*, Sci. Rep., 2012.

[8] F. Darabi Sahneh and C. Scoglio, Epidemic spread in human networks, in *50th IEEE Conference on Decision and Control and European Control Conference (CDC-ECC)*, (2011), 3008–3013.

[9] F. Darabi Sahneh and C. Scoglio, Optimal information dissemination in epidemic networks, in *51st Annual Conference on Decision and Control (CDC), IEEE*, (2012), 1657–1662.

[10] M. Dickison, S. Havlin and H. E. Stanley, Epidemics on interconnected networks, *Physical Review*, **85** (2012), 066109.

[11] R. Diestel, *Graph Theory*, Springer Graduate Texts in Mathematics (GTM), 2012.

[12] S. Funk and V. A. Jansen, Interacting epidemics on overlay networks epidemic spreading in multiplex networks, *Physical Review*, **81** (2010), 036118.

[13] A. Ganesh, L. Massoulie and D. Towsley, The effect of network topology on the spread of epidemics, in *INFOCOM 2005. 24th Annual Joint Conference of the IEEE Computer and Communications Societies. Proceedings IEEE*,**2** (2005), 1455-1466.

[14] C. Granell, S. Gómez and A. Arenas, Dynamical interplay between awareness and epidemic spreading in multiplex networks, *Physical review letters*, **111** (2013), 128701.

[15] M. C. Grant, S. Boyd and Y. Ye, CVX: Matlab software for disciplined convex programming (web page and software), Available from: `http://cvxr.com/cvx`.

[16] J. Kuczynski and H. Wozniakowski, Estimating the largest eigenvalue by the power and Lanczos algorithms with a random start, *SIAM journal on matrix analysis and applications*, **13** (1992), 1094–1122.

[17] B. Lemmens and R. Nussbaum, *Nonlinear Perron-Frobenius Theory*, Cambridge University Press, 2012.

[18] Y. Nesterov, Smoothing technique and its applications in semidefinite optimization, *Science*, **110** (2007), 245–259.

[19] Y. Nesterov and A. Nemirovskii, *Interior-point Polynomial Algorithms in Convex Programming*, Society for Industrial and Applied Mathematics, 1994.

[20] M. Penrose, *Random Geometric Graphs*, Oxford University Press, 2003.

[21] V. M. Preciado, D. Sahneh and C. Scoglio, A convex framework for optimal investment on disease awareness in social networks, in *Global Conference on Signal and Information Processing (GlobalSIP), IEEE*, (2013), 851–854.
[22] A. Saumell-Mendiola, M. A. Serrano and M. Bogu, Epidemic spreading on interconnected networks, *Physical Review*, **86** (2012), 026106.
[23] P. Schumm, W. Schumm and C. Scoglio, Impact of Preventive Responses to Epidemics in Rural Regions, *PloS one*, **8** (2013), e59028.
[24] G. Sun, Pattern formation of an epidemic model with diffusion, *Nonlinear Dyn*, **69** (2012), 1097–1104.
[25] G. Sun, Q. Liu, Zh. Jin, A. Chakraborty and B. Li, Influence of infection rate and migration on extinction of disease in spatial epidemics, *Journal of Theoretical Biology*, **264** (2010), 95–103.
[26] P. Van Mieghem, The N-intertwined SIS epidemic network model, *Computing*, **93** (2011), 147–169.
[27] P. Van Mieghem, J. Omic and R. Kooij, Epidemic Thresholds in Real Networks, *IEEE/ACM Transactions on Networking*, **17** (2009), 1–14.
[28] O. Yağan and V. Gligor, Analysis of complex contagions in random multiplex networks, *Physical Review*, **86** (2012), 036103.

Received August 01, 2014; Accepted December 23, 2014.

E-mail address: heman@ksu.edu
E-mail address: faryad@ksu.edu
E-mail address: pietro@math.ksu.edu
E-mail address: preciado@seas.upenn.edu
E-mail address: caterina@ksu.edu